Proof

Full Paper

Multistep Surface Electrode Mechanism Coupled with Preceding Chemical Reaction-Theoretical Analysis in Square-Wave Voltammetry

Milkica Janeva, Pavlinka Kokoskarova, and Rubin Gulaboski*

Faculty of Medical Sciences, „Goce Delcev" University, Stip, Macedonia

*Corresponding Author, Tel.:;Fax:

E-Mail: rubin.gulaboski@ugd.edu.mk

Abstract- In this theoretical work, we present for the first time voltammetric results of a surface multistep electron transfer mechanism that is associated with a preceding chemical reaction that is linked to the first electron transfer step. The mathematical model of this so-called "surface CEE mechanism" is solved under conditions of square-wave voltammetry. We present relevant set of results portraying the influence of kinetics and thermodynamics of chemical step to the features of simulated voltammograms. In respect to the potential difference at which both electrode processes occur, we consider two different situations. In the first scenario, both peaks are separated for at least |150 mV|, while in the second case both peaks occur at same potential. Under conditions when both peaks are separated for at least |150 mV|, the first process can be described with the voltammetric features of a surface CE mechanism, while the second peak gets attributes of a simple surface electrode reaction. When both peaks take place at same potential, we elaborate an elegant methodology to achieve separation of both overlapped peaks. This can be done by modifying the concentration of the substrate "Y" in electrochemical cell that is involved in the preceding chemical reaction. The results of this work can be of big assistance to experimentalists working in the field of voltammetry of metal complexes and drug-drug interactions.

Keywords-Two-step surface reactions; Protein-film voltammetry; CEE mechanism; Kinetics of homogenous chemical reaction; Equilibrium constant

1 **1. INTRODUCTION**

2   The voltammetric determination of kinetic and thermodynamic parameters that are related
3 to interaction between biomolecules, particularly when these are immobilized on a given
4 substrate, attracts considerable interest in the last 30 years [1-7]. Electrochemical systems in
5 which at least one participant is adsorbed at the working electrode surface are commonly
6 defined as "surface redox reactions" [1, 3, 4, 8]. If voltammetry of lipophilic redox enzymes
7 is considered, then the voltammetric technique that allows studying the redox chemistry of
8 such systems is named "protein-film voltammetry" [5, 8-10]. Relevant experimental
9 examples belonging to surface redox systems are found in antibody-antigen recognition [6],
10 drug-drug interactions [11], recognition of single-stranded DNA [6, 7] and in interactions of
11 many physiological molecules [1, 3, 6]. To get a voltammetric access to parameters that are
12 relevant to thermodynamics and kinetics of surface-active redox substances, we have to
13 monitor the changes in surface concentration of defined substrates analyzed under conditions
14 of applied potential. However, before we consider a suitable voltammetric procedure for such
15 an analysis, we must determine the exact nature of electrochemical mechanism going on in
16 electrochemical cell. The last is of outmost importance in order to apply adequate method for
17 getting access to kinetics and thermodynamics related to defined system of interest. In the last
18 30 years, the square-wave voltammetry (SWV) is recognized as a powerful pulse
19 voltammetric technique that enables studying the redox mechanisms of many surface redox
20 reactions, and enzymatic reactions as well [1, 3, 5, 8-10]. In addition, it provides elegant
21 means to access relevant kinetics and thermodynamics parameters of important surface redox
22 systems [1-8]. As many surface-active biomolecules exhibit electrochemical activity in a
23 multielectron multi-step fashion [4-7], it was very important to develop theoretical models of
24 such systems under conditions of SWV. In [12-18] we reported on important theoretical
25 models of surface multistep mechanisms associated with follow-up and regenerative chemical
26 reactions under conditions of SWV. In this work, we report for the first time a voltammetric
27 theory of multielectron two-step surface redox mechanism that is associated with preceding
28 chemical reaction under conditions of SWV. The abbreviation of this particular electrode
29 mechanism is a "surface CEE mechanism". Importance of this particular mechanism is seen
30 in the redox chemistry of many metal-ligand complexes [19] and complex biomolecules as
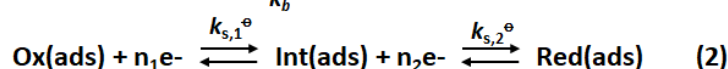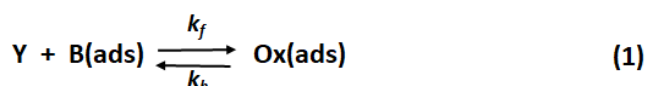31 described in [3-7].

32

33 **2. EXPERIMENTAL**

34 **2.1. Mathematical model**

35   Surface electrode mechanism comprising two successive electron transfers, associated
36 with a preceding chemical reaction that is linked to the first electrode step is elaborated
37 theoretically under conditions of square-wave voltammetry. The electrochemical abbreviation

1   of this complex system is a "surface CEE" mechanism. With term "E" we define a given
2   electron transfer step, while the term "C" stands to describe to a reversible chemical reaction.
3   We assume that all electrochemically active species are strongly and uniformly immobilized
4   to the surface of the working electrode. In the first step (1), we assume occurrence of a
5   reversible chemical reaction between electrochemically inactive species Y and B(ads) that
6   generates the initial electroactive species Ox(ads). The electrochemical transformation of
7   Ox(ads) to Red(ads) takes place in two consecutive one-electron steps (2). Schematically, this
8   mechanism can be described as follows:
9

$$Y + B(ads) \underset{k_b}{\overset{k_f}{\rightleftharpoons}} Ox(ads) \qquad (1)$$

$$Ox(ads) + n_1 e^- \overset{k_{s,1}^{\ominus}}{\rightleftharpoons} Int(ads) + n_2 e^- \overset{k_{s,2}^{\ominus}}{\rightleftharpoons} Red(ads) \qquad (2)$$

10
11

12   Only the species "B(ads)" and "Y" are present in the electrochemical cell before potential
13   is applied. We assume that all immobilized species are uniformly adsorbed ("ads") at the
14   surface of the working electrode and there are no any lateral interactions between the
15   adsorbed species. "Int(ads)" stands for an electroactive substrate that is formed
16   electrochemically as an intermediate in the first electrode reduction step. With "Red(ads)" we
17   assign the final redox-active species, which is generated electrochemically during the second
18   electrode transfer step from Int(ads). "Y" is a symbol of the substrate that should be present
19   in large excess in the electrochemical system, and it shows no electrochemical activity in the
20   potential region explored in the voltammetric experiment. We assume that "Y" reacts
21   selectively and in chemically reversible manner with B(ads) species, while generating the
22   initial electro-active species Ox(ads). Mathematically, the elaborated surface CEE
23   mechanism in this work can be represented with following equations:
24
25    $t = 0$; $\Gamma(B) = \Gamma^*(B)$; $\Gamma(Ox) = K_{eq}\,\Gamma^*(B)$; $\Gamma(Red) = 0$ $\qquad$ (a)

26    $t > 0$; $\Gamma(B) + \Gamma(Ox) + + \Gamma(Int) + \Gamma(Red) = \Gamma^*(B)$; $K_{eq} = k_f/k_b$; $\qquad$ (b)

27   For t > 0, the differential equations (c-f) link the changes of surface concentrations with
28   the faradaic current and the kinetics and thermodynamics of preceding chemical step:
29
30    $(d\Gamma(B)/dt) = k_b\Gamma(Ox) - k_f\Gamma(B)$ $\qquad$ (c)

31    $d\Gamma(Ox)/dt = -I_1/(n_1 FS) - k_b\Gamma(Ox) + k_f\Gamma(B)$ $\qquad$ (d)

32    $d\Gamma(Int)/dt = I_1/(n_1 FS) - I_2/(n_2 FS)$ $\qquad$ (e)

33    $d\Gamma(Red)/dt = I_2/(n_2 FS)$ $\qquad$ (f)

1   The mutual dependence between the electric current, electrical potentials, the surface

2   concentrations of electrochemically active species, and the kinetic parameters relevant to both

3   electron transfer steps is achieved via the Butler-Volmer equations having following forms:

4

5    $(I_1/n_1FS) = k_{s,1}^{\ominus}\exp(-\alpha\Phi_1)\,[\Gamma(\text{Ox}) - \exp(\Phi_1)\,\Gamma(\text{Int})]$ (g)

6    $(I_2/n_2FS) = k_{s,2}^{\ominus}\exp(-\alpha\Phi_2)\,[\Gamma(\text{Int}) - \exp(\Phi_2)\,\Gamma(\text{Red})]$ (h)

7   In the Supplementary of this work we provide the readers entire MATHCAD working

8   sheet containing all recurrent formulas and parameters needed for simulation of the

9   theoretical voltammograms of the surface CEE mechanism. In all simulation voltammetric

10   patterns, we defined the reduction currents to have positive value (blue color), and negative

11   sign is ascribed to oxidation currents (represented with red color). Net SWV currents are

12   assigned with black color at all simulated patterns. It is important to note that we defined all

13   potentials against the standard redox potential of the first electrode process (defined as "Peak

14   I" in this work). In all calculations, we set the starting potential to defined positive value, and

15   the scan is directed towards negative final potentials.

16

17   **2.2. Definition of the parameters that exhibit effect to the relevant characteristics of**

18   **calculated square-wave voltammograms**

19   With the equation $\Psi = \Psi_I + \Psi_{II}$ is defined the net dimensionless current of theoretical SW

20   voltammograms that is as a sum of the particular currents related to the first and the second

21   electrode step, respectively. These particular currents are defined as $\Psi_I = I_1/[(n_1FSf\Gamma^*)]$ and

22   $\Psi_{II} = I_2/[(n_2FSf\Gamma^*)]$. Symbol "I" stands for the faradaic electric current of first (I_1) and second

23   (I_2) electrode process, while n_1 and n_2 refer to number of electrons involved in each electrode

24   step. Symbol S stands for the active area of the working electrode, while with f we define the

25   frequency of SW pulses, $f = 1/(2t_p)$. In last equation, t_p is the time of duration of a single

26   potential pulse in SWV. With Γ^* we assign the total surface concentration, which is actually

27   equal to the initial surface concentration of adsorbed B(ads) species. Φ stays for the

28   dimensionless potentials that are defined as $\Phi_1 = nF(E - E_1^{\ominus}/RT)$ and $\Phi_2 = nF(E - E_2^{\ominus}/RT)$,

29   for the first and the second electrode process, respectively. In last two equations, $E_1^{\ominus}$ and $E_2^{\ominus}$

30   are symbols for the standard potentials of the first and the second electron transfer step,

31   respectively. With "α" we assign the coefficient of electron transfer that was set to $\alpha = 0.5$ for

32   both EE steps. T is a symbol of the thermodynamic temperature (T = 298 K in all

33   simulations), R is the universal gas constant, and F is the Faraday constant. The features of

34   theoretical SW voltammograms are also function of several dimensionless parameters. The

35   dimensionless kinetic parameters $K_I = k_{s,1}^{\ominus}/f$ and $K_{II} = k_{s,2}^{\ominus}/f$ portray the effect of $k_{s,1}^{\ominus}$ and

36   $k_{s,2}^{\ominus}$ (i.e. the standard kinetic constants of both EE processes) to the duration of the SW

37   potential pulses. In addition, the major attributes of theoretical SW voltammograms are

1   affected by a dimensionless chemical parameter $K_{chemical}$, defined as $K_{chemical} = \varepsilon/f$. In last
2   equation, $\varepsilon = (k_f + k_b)$ is the cumulative chemical parameter defined as a sum of the first order
3   rate constant k_f and k_b of the forward and backward chemical reactions, respectively. $K_{chemical}$
4   reflects the overall rate of the chemical step relative to the time-frame of current
5   measurement in SWV. Since we assume to have substrate "Y" that should be present in very
6   large excess in the electrochemical cell, then it holds true that chemical parameter $K_{chemical}$ is
7   of pseudo-first order. It depends on the concentration of substrate "Y" -$c(Y)$ via following
8   relationship: $\varepsilon = [k_f^{\ominus}c(Y) + k_b]$. In the last equation, $k_f^{\ominus}$ is the real rate constant of forward
9   chemical step. In addition, the features of calculated SW voltammograms are function of the
10 equilibrium constant K_{eq} that is defined as $K_{eq} = k_f/k_b$. The magnitude of chemical equilibrium
11 constant determines the quantity of Ox(ads) that is available to undergo electrode
12 transformation. In all simulations, we set the parameters of the applied bias to following
13 constant values: frequency $f = 10$ Hz, amplitudeof the SW pulses $E_{sw} = 50$ mV, and potential
14 increment $dE = 10$ mV. Additional material for the algorithms used in this work is provided
15 in the *Supplementary* of this work and in our works [1, 13]. For all simulations, we used
16 commercially available software MATHCAD 14.
17
18 **3. RESULTS AND DISCUSSION**
19   The voltammetric complexity of multistep surface mechanisms can be initially simplified
20 if we assume that both peaks are separated for at least |150 mV|. Under such circumstances,
21 the voltammetric patterns of a surface CEE mechanism are equivalent to the SW
22 voltammograms simulated for a surface EE mechanism [20], when the equilibrium constant
23 $K_{eq} > 10$, independent on the magnitude of dimensionless chemical parameter $K_{chemical}$ [1, 21].
24 In this scenario, the chemical equilibrium is shifted significantly to the right, i.e. towards
25 production of initial electrochemically active species Ox(ads). Under such conditions, one
26 can explore the methods reported in [1, 20] to get access to the kinetic and thermodynamic
27 parameters relevant to both electron transfer steps. When $K_{eq} \leq 1$, then we witness significant
28 effects of equilibrium constant and dimensionless chemical parameter to the features of
29 calculated SW voltammograms. In Figure 1 we present several calculated SW
30 voltammograms of a surface CEE mechanism portraying the effect of the rate of preceding
31 chemical step. SW voltammograms are simulated for $K_I = K_{II} = 1.6$, and for magnitude of K_{eq}
32 = 0.5. As expected, magnitude of $K_{chemical}$ shows effect to the features of "Peak I" only, which
33 gets shapes as typical of a surface CE mechanism [1, 21]. For $K_{chemical} \geq 10$, there is no further
34 influence of chemical reaction rate to the features of simulated SWV patterns, and entire
35 system turns to a two-step surface EE mechanism [20].
36   Presented in Figure 2a-b is the effect of $K_{chemical}$ to the magnitude of net SWV peak
37 currents and net SWV peak potentials of "Peak I". Curves are calculated for $K_I = 0.2$, and for
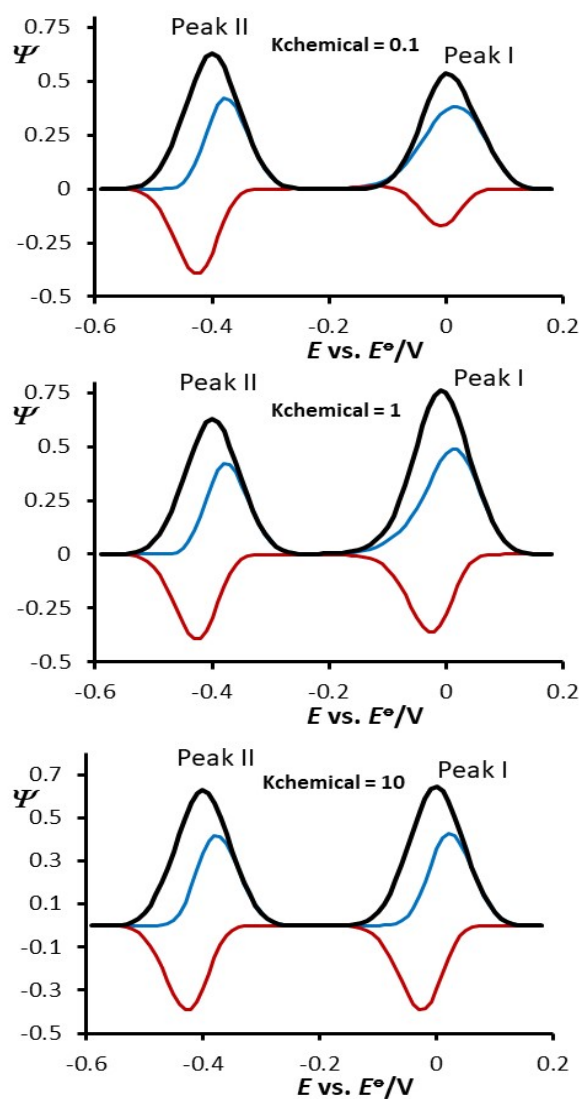38 three different magnitudes of K_{eq}.

Figure 1. Influence of the dimensionless chemical parameter $K_{chemical}$ to the features of SW voltammograms simulated for $K_I = K_{II} = 1.60$, and equilibrium constant of $K_{eq} = 0.5$. The potential separation between both peaks is set to |400 mV|. The values of other parameters used in simulations were: temperature $T = 298$ K; number of electrons $n_1 e^- = n_2 e^- = 1$; electron transfer coefficient $\alpha = 0.5$, potential step $dE = 10$ mV, frequency $f = 10$ Hz. The values of $K_{chemical}$ are given in the charts.

A sigmoidal dependence exists between the net SWV peak current of "Peak I" - $\Psi_{net,p1}$ and the $\log(K_{chemical})$, with a linear "kinetic zone" existing roughly in the region $-1 < \log(K_{chemical}) < 1$ (Figure 2a). Indeed, the region in which we "detect" a linear kinetic effect of $\log(K_{chemical})$ to $\Psi_{net,p1}$ depends on magnitude K_{eq}, and it is larger at smaller values of K_{eq}. The shift of the net-SW potential of "Peak I" as a function of logarithm of chemical kinetic parameter also follows a sigmoidal dependence (Figure 2b).
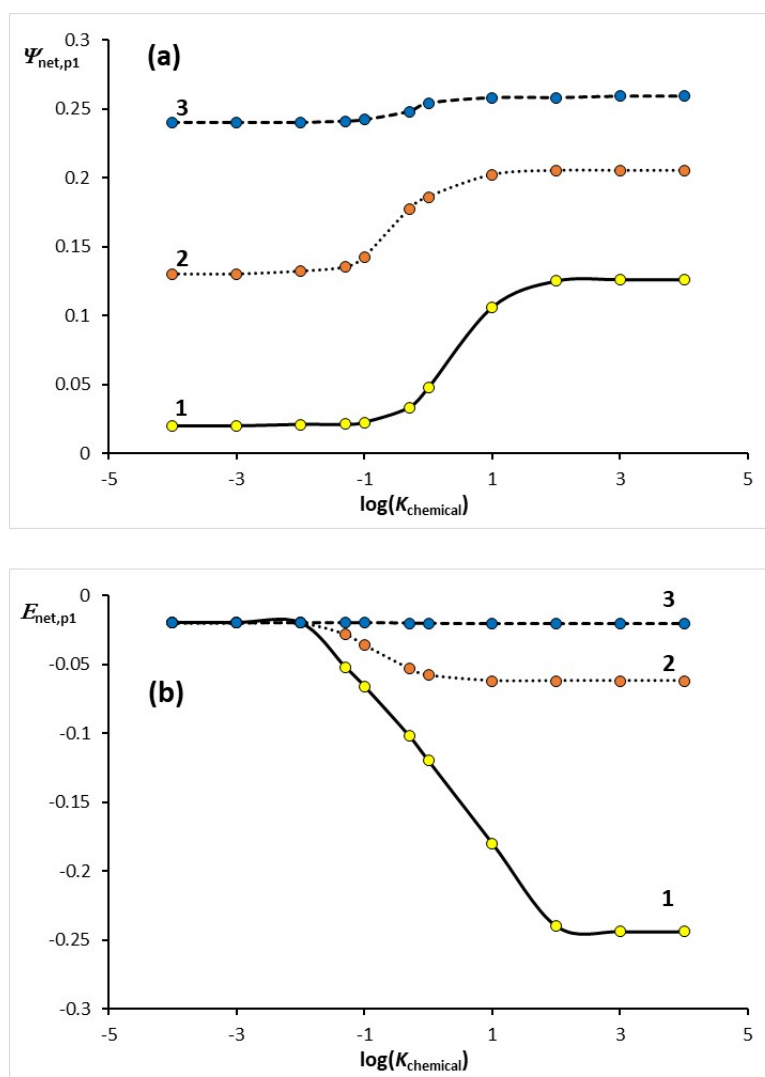
1

2   **Figure 2.** Effect of dimensionless chemical rate parameter $K_{chemical}$ to the net peak currents

3    $\Psi_{net,p1}$ (a) and the net peak-potentials $E_{net,p1}$ (b) of SW voltammograms of "Peak I".

4   Voltammograms are simulated at $K_I = 0.2$ and $K_{eq} = 0.1$ (1); 1 (2) and 10 (3). The other

5   parameters used in simulation were same as those in Figure 1.

6

7   For $K_{eq} \leq 1$, we observe linear parts of the dependence $E_{net,p1}$ *vs.* log($K_{chemical}$), roughly in

8   the regions $-1 < $ log($K_{chemical}$) $ < 1.5$. The slope of the linear parts of the curves $E_{net,p1}$ *vs.*

9   log($K_{chemical}$) is a function of K_{eq} and it is defined as **2.303[RT/F]log[K_{eq}/(1+K_{eq})]**. Therefore,

10   the magnitude of the slope of $E_{net,p1}$ *vs.* log($K_{chemical}$) can be explored for the determination of

11   the value of K_{eq}. The dependences between $\Psi_{net,p1}$ and $E_{net,p1}$ as a function of K_{eq} are

12   presented in Figure 3a-b. Curves are simulated for $K_I = K_{II} = 0.2$, and for three different

13   values of $K_{chemical}$. All curves of the dependence of $\Psi_{net,p1}$ *vs.* log(K_{eq}) have a sigmoidal shape

14   with identical slopes of the linear parts (Figure 3a). For magnitudes of log(K_{eq}) > 2, we detect

15   a constant value of $\Psi_{net,p1}$, independent on K_{eq}.

16
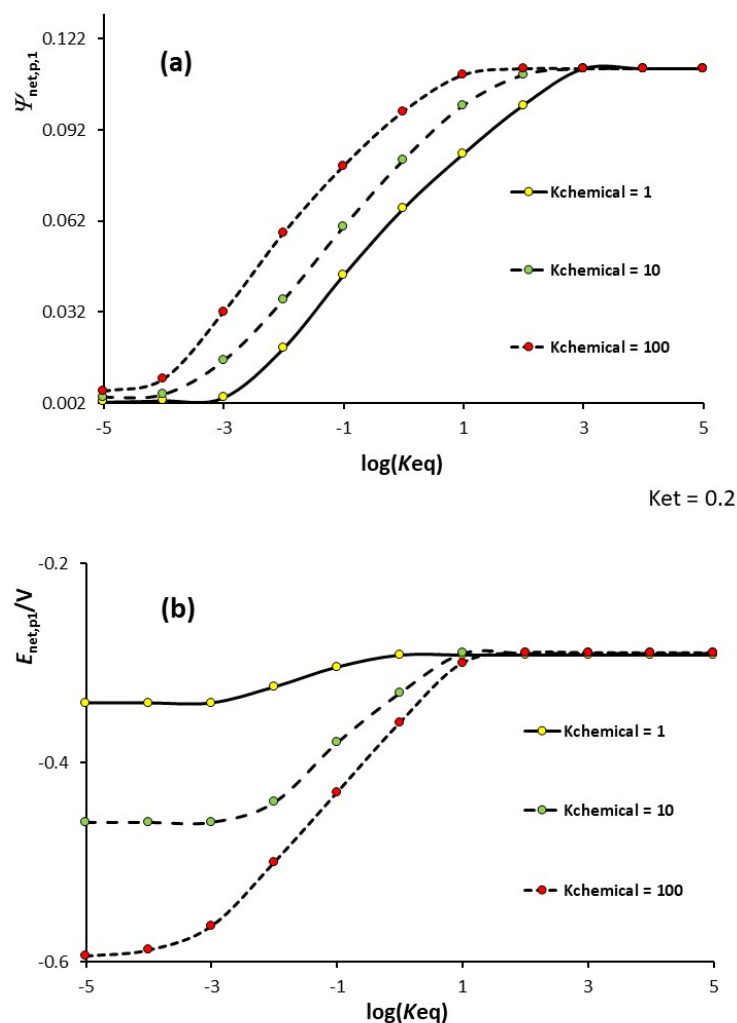
Figure 3. Influence of the equilibrium constant of preceding chemical reaction K_{eq} to the net peak currents $\Psi_{net,p1}$ (a) and the net peak-potentials $E_{net,p1}$ (b) of SW voltammograms of "Peak I". Voltammograms are simulated at $K_I = 0.2$ and $K_{chemical} = 1$, 10 and 100. The other parameters used in simulation were same as those in Figure 1.

This scenario corresponds to significant shift of the chemical equilibrium towards Ox(ads) species, which turns the features of first peak ("Peak I") from CE to a simple E mechanism [21]. The dependence of the magnitude of net SWV peak potential of "Peak I"-$E_{net,p1}$ as a function of $\log(K_{eq})$ also follows a sort of sigmoidal function (Figure 3b). In general, an increase of K_{eq} generates a shift of $E_{net,p1}$ towards more positive values. For $\log(K_{eq}) > 1$, the net SWV peak potential of "Peak I" is independent on K_{eq}. The slopes of the linear segments of the dependences $E_{net,p1}$ *vs*. $\log(K_{eq})$ are function of $K_{chemical}$, and they get steeper at higher values of chemical rate parameter. A typical feature of all surface mechanisms in pulse voltammetric techniques is the so-called "quasireversible maximum". A sort of parabolic dependence of net SWV peak currents and the logarithm of electrode kinetic parameter exists, as a result of the synchronization of the kinetics of electron transfer to the time-frame

1   of current measurements in SWV [1, 22]. This phenomenon can be used for the estimation of
2   standard rate constant of electron transfer step in a very simple manner [1]. As reported in
3   [21, 23], for a surface CE mechanism, the position of the "quasireversible maximum" is not
4   affected by the kinetics of chemical reaction that precedes the electron transfer step.
5   Therefore, this feature can be used for accurate assessment of both $k_{s,1}^{\ominus}$ and $k_{s,2}^{\ominus}$
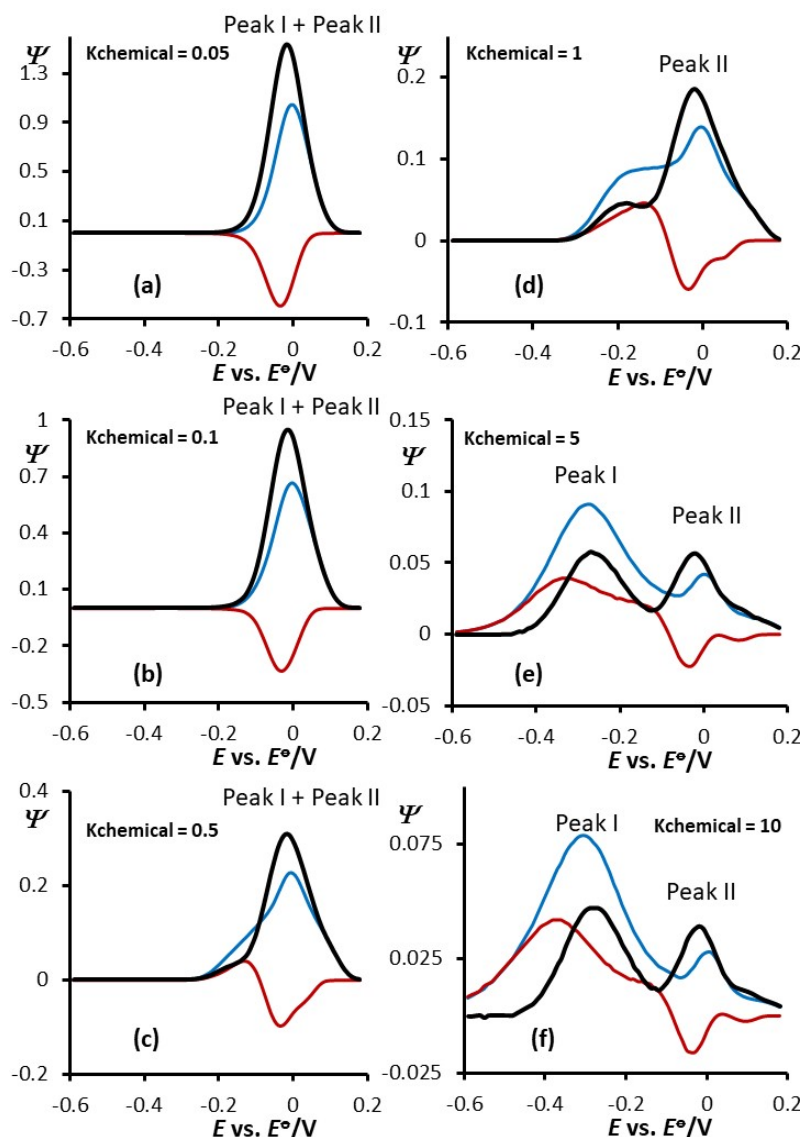6   independently for both SWV peaks of a surface CEE mechanism.
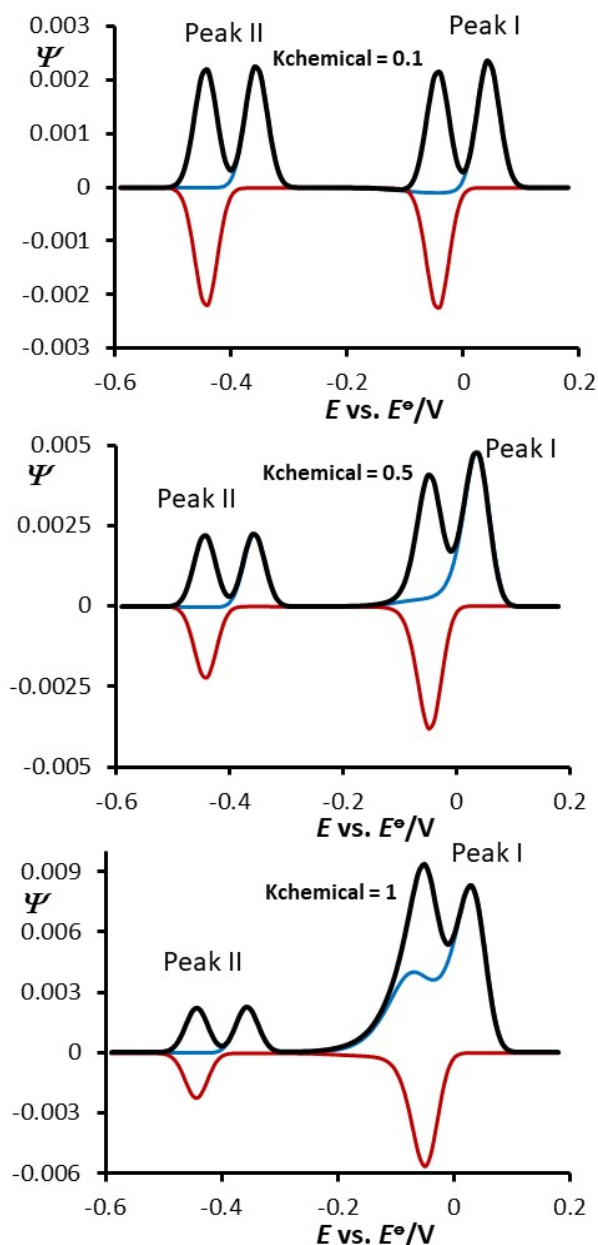
7
8   **Figure 4.** Influence of the dimensionless chemical parameter $K_{chemical}$ to the features of SW
9   voltammograms in situation of fast electron transfer at both electrode steps. Voltammetric
10   patterns are simulated for $K_I = K_{II} = 10$, and equilibrium constant of $K_{eq} = 0.1$. The potential
11   separation between both peaks is set to |400 mV|. The values of $K_{chemical}$ are given in the
12   charts. Other simulation conditions are same as those in Figure 1.

1   When the kinetics of electron transfer is very fast (see Figure 4a), then one might witness a
2   phenomenon of so-called "split net SWV peaks" [1, 22, 24]. In such scenario, a very short
3   time-frame at SW potential pulses is needed for the electrochemical conversion of redox
4   active form Ox(ads) to redox form Red(ads). However, an electrochemical conversion of
5   Ox(ads) to Red(ads) also happens in the so-called "dead time" (i.e. the time segment in which
6   faradaic current is not measured) of SW pulses [1, 22]. Therefore, in the small time-frame
7   where electrical current is measured at the defined SW pulses, only very small amounts of
8   Ox(ads) (or Red) will be available for electrochemical transformation. Such a phenomenon
9   will be portrayed in small faradaic currents measured in SWV of surface electrochemical
10   systems that features very fast rate of electrode steps [24]. As the rate of electrode reaction
11   gets faster, then the reduction process shifts towards more positive potentials, while the
12   oxidation process moves to more negative potentials. This will result in a splitting of the net
13   SWV peak in two symmetric peaks, whose characteristics can be used to determine the
14   magnitude of $k_s^{\ominus}$ as elaborated in [1, 24]. Shown in figure 4b-d is the effect of chemical rate
15   parameter $K_{chemical}$ to the features of calculated patterns in scenario of "split SW peaks" of a
16   surface CEE mechanism. Voltammograms are simulated for $K_I = K_{II} = 10$, and for $K_{eq} = 0.1$.
17   As the second process at more negative potentials (Peak II) remains unaffected by $K_{chemical}$,
18   the features of first SWV process (Peak I) get significantly affected by the value of $K_{chemical}$.
19   An increase of $K_{chemical}$ from 0.1 to 1 is followed by a rise of all current components of "Peak
20   I". In same direction, we witness a diminishment of the potential separation between the split
21   patterns of net "Peak I". For $K_{chemical} > 2$, the splitting phenomenon vanishes and only a
22   single-featured "peak I" exists at more positive potentials, with intensity that is much higher
23   than that of "Peak II" (not shown). The phenomena portrayed in figure 4 can be used as a
24   qualitative criterion to recognize the surface CEE mechanism, if both SWV peaks are
25   separated for at least |150 mV|.
26   When both SWV peaks, which represent both electrode reactions of a defined multistep
27   electron transfer process, are separated for at least |150 mV|, then it becomes quite easy to
28   achieve independent estimation of all relevant parameters to both electrode steps [12, 23].
29   However, when both EE steps occur at a same potential, then the CEE electrode mechanism
30   will be portrayed in a single SW voltammogram that "hides" all processes in it (figure 5a). In
31   such scenario, it is a challenging task to determine whether the obtained single SWV peak is
32   a consequence of a simple two-electron transfer that occurs in one step, or it is due to
33   occurrence of two successive electron transfers. In our recent paper [25], we have shown that
34   in a surface EEC mechanism studied with SWV, there is a simple way to determine
35   occurrence of a two-step successive surface electrode mechanism, when both EE steps take
36   place at equal potential. It has been shown that at an increased rate of the chemical reaction
37   that follows the electron transfer step, expressed via $K_{chemical}$, can lead to displacement of the
38   second electrode step of a surface EECrev mechanism to positive potentials. Similar

algorithm can also be applied to recognize a surface CEE mechanism, when both EE processes are defined to take place at a very same potential. In this case, an increased rate of the preceding chemical reaction displaces the first electron transfer process towards more negative potentials (Figure 5b-f). For $K_{eq} = 0.1$, and $K_I = K_{II} = 1.6$, a simple separation of both electron transfers (that happen at very same potential) can be achieved for $K_{chemical} \geq 5$ (see Figure 5e-f). This feature can be explored as additional diagnostic criterion for recognizing the surface CEE mechanism. Therefore, one can use this characteristic for separation of both EE processes of a CEE mechanism, and to analyze them independently, if both happen at the same potential.

Figure 5. Influence of the magnitude of dimensionless chemical parameter $K_{chemical}$ to the features of SW voltammograms in situation when both electrode processes take place at same potential. SW voltammetric patterns are simulated for $K_{eq} = 0.1$, and $K_I = K_{II} = 1.60$. The values of $K_{chemical}$ are given in the charts. Other conditions are same as in Figure 1.

1 **4. CONCLUSION**

2   The results presented in this work enable a comprehensive study of the voltammetric
3   responses of a surface CEE mechanism as a function of the kinetic rate constant and
4   equilibrium constant of preceding chemical step. From the voltammograms simulated in this
5   work, we can observe that the kinetic and thermodynamic parameters associated to chemical
6   step can exhibit rather complex behavior to simulated SW voltammograms. Even more
7   complex situation is met if both electron transfers take place at same electrode potential.
8   When both electrode steps of a surface CEE mechanism occur at potentials that are at least
9 |150 mV| separated from each other, then one can explore independent methodologies to
10 determine the relevant rate constant and equilibrium constant of both electrode steps. For
11 both EE steps, one can explore the phenomenon "quasireversible maximum" [1] and "split
12 net SWV peaks" [24] to get access to the magnitudes of $k_{s,1}^{\ominus}$ and $k_{s,2}^{\ominus}$. Under such
13 circumstances, the methods reported in [1, 20, 23] can be used to access the kinetics and
14 thermodynamic parameters related to the preceding chemical reaction. For these estimations,
15 one needs the value of electron transfer coefficient that can be evaluated by using the method
16 reported in [26]. If both EE processes occur at same potential, a crucial point is to recognize
17 whether the electrode step is a single electron transfer, or it is a consequence of two one-step
18 reactions. As we elaborated in this work, at given magnitudes of K_{eq}, K_I and K_{II}, all relevant
19 characteristics of simulated SWV paterns of a surface CEE mechanism are function of the
20 dimensionless chemical parameter $K_{chemical}$. For $K_{eq} \leq 1$, an increase of $K_{chemical}$ leads to a shift
21 of the position of first electrode step towards more negative potentials. As presented in figure
22 5e-f, at given critical value of $K_{chemical}$, we can achieve separation of both EE processes
23 defined to take place at same potential. In the section "Mathematical model" of this work, it
24 is explicitly shown that the dimensionless chemical parameter $K_{chemical}$ depends on
25 concentration of "Y"-c(Y) and the frequency f. It is important to mention that f affects in the
26 same time the kinetics of chemical reactions, and the rate of the electrochemical reactions
27 (via K_I and K_{II}) of the redox active compounds. Therefore, the frequency analysis in real
28 experiments of such systems will produce a rather complex interplay to all relevant kinetic
29 parameters. So, a more relevant protocol to achieve experimentally the separation of both
30 peaks of SW voltammograms portrayed in figure 5 is to make modification of the molar
31 concentration of substrate "Y". In such experiments, we should keep at constant values the
32 SW frequency, and also the SW amplitude and the potential step [27]. From the experimental
33 voltammograms obtained by modifying the molar concentration of substrate "Y" only, we
34 can distinguish the elaborated surface CEE from other surface mechanisms (two-step) that are
35 associated with chemical reactions. This is achievable, because all other multistep surface
36 mechanisms coupled with chemical reactions (i.e., ECE, EEC and EEC' mechanisms) [12-18,
37 25] show very specific SW voltammetric characteristics, regardless if both EE processes
38 occur at a very same or at quite different potentials.

Acknowledgments

All authors thank the "Goce Delcev" University in Stip, Macedonia for the support. This article is in memory of our great friend and collaborator, Prof. Dr. Sci. Šebojka Komorsky-Lovrić.

REFERENCES

[1]   V. Mirceski, S. Komorsky-Lovric, and M. Lovric, Square-wave voltammetry, Theory and application (F. Scholz, ed.), Springer, Berlin, Germany (2007).

[2]   A. Molina, and J. Gonzales, Pulse voltammetry in physical electrochemistry and electroanalysis, in Monographs in electrochemistry (F. Scholz, ed.), Berlin Heidelberg, Springer (2016).

[3]   R. G. Compton, and C. E. Banks, Understanding voltammetry, 2nd Edition, Imperial College Press, London, UK (2011).

[4]   A. J. Bard, and L. R. Faulkner, Electrochemical methods. Fundamentals and applications, 3rd edition, John Wiley & Sons, Inc. (2004).

[5]   F. A. Armstrong, Voltammetry of Proteins. In: A. J. Bard, M. Stratmann, G. S. Wilson (eds) Encyclopedia of Electrochemistry, vol. 9, Wiley VCH, Weinheim (2002).

[6]   P. N. Barlett, Bioelectrochemistry-Fundamentals, Experimental Techniques and Application, Wiley, Chichester (2008).

[7]   M. Saveant, Elements of Molecular and Biomolecular Electrochemistry: An Electrochemical Approach to Electron Transfer Chemistry, Hoboken, NJ, Wiley (2006).

[8]   V. Mirceski, R. Gulaboski, M. Lovric, I. Bogeski, R. Kappl, and M. Hoth, Electroanalysis 25 (2013) 241.

[9]   C. Léger, and P. Bertrand, Chem. Rev. 108 (2008) 2379.

[10] R. Gulaboski, V. Mirceski, I. Bogeski, and M. Hoth, J. Solid State Electrochem. 16 (2012) 2315.

[11] R. Gulaboski, P. Kokoskarova, and S. Petkovska, Anal. Bioanal. Electrochem. 12 (2020) 345.

[12] M. Janeva, P. Kokoskarova, V. Maksimova, and R. Gulaboski, Electroanalysis 31 (2019) 2488.

[13] R. Gulaboski, J. Solid State Electrochem. 13 (2009) 1015.

[14] R. Gulaboski, and L. Mihajlov, Biophys. Chem. 155 (2011) 1.

[15] V. Mirceski, and R. Gulaboski, Maced. J. Chem. Chem. Eng. 33 (2014) 1.

[16] P. Kokoskarova, M. Janeva, V. Maksimova, and R. Gulaboski, Electroanalysis 31 (2019) 1454.

[17] P. Kokoskarova, and R. Gulaboski, Electroanalysis 32 (2020) 333.

[18] R. Gulaboski, P. Kokoskarova, and S. Mitrev, Electrochim. Acta 69 (2012) 86.

[19] A. Lasia, Can. J. Chem. 64 (1986) 2319.

1 [20] V. Mirceski, and R. Gulaboski, Croat. Chem. Acta 76 (2003) 37.
2 [21] R. Gulaboski, V. Mirceski, M. Lovric, and I. Bogeski, Electrochem. Commun. 7 (2005)
3   515.
4 [22] R. Gulaboski, Electroanalysis 31 (2019) 545.
5 [23] R. Gulaboski, V. Mirceski, and M. Lovric, J. Solid State Electrochem. 23 (2019) 2493.
6 [24] V. Mirceski, and M. Lovric, Electroanalysis 9 (1997) 1283.
7 [25] R. Gulaboski, and V. Mirceski, J. Solid State Electrochem. 24 (2020) doi:
8   10.1007/s10008-020-04563-9
9 [26] R. Gulaboski, M. Lovric, V. Mirceski, I. Bogeski, and M. Hoth, Biophys. Chem. 138
10   (2008) 130.
11 [27] V. Mirceski, L. Stojanov, and B. Ogorevc, Electrochim. Acta 327 (2019) 134997.

12
13
14
15
16
17
18
19
20
21
22
23
24
25
26
27
28
29
30
31
32
33
34
35